ChemComm
Chemical Communications

Accepted Manuscript

This article can be cited before page numbers have been issued, to do this please use: E. Luneva, F. Aribot, J. E. McPeak, K. S. Pedersen, M. A. Dunstan, N. J. Yutronkie, A. Rogalev and G. Nocton, *Chem. Commun.*, 2025, DOI: 10.1039/D5CC04048E.

ROYAL SOCIETY OF CHEMISTRY

rsc.li/chemcomm

View Article Online
DOI: 10.1039/D5CC04048E

Journal Name

ARTICLE TYPE

Cite this: DOI: 00.0000/xxxxxxxxxx

4f-intermediate valence in an ytterbium–bipyridine coordination solid†

Evgeniia Luneva,[a] Maja A. Dunstan,*[a] Frédéric Aribot,[a] Nathan J. Yutronkie,[b] Joseph E. McPeak,[c] Andrei Rogalev,[b] Grégory Nocton,[d] and Kasper S. Pedersen*[a]

Received Date
Accepted Date

DOI: 00.0000/xxxxxxxxxx

We report the first structurally characterised coordination solids based on decamethylytterbocene, using bipyridine linkers to form $YbCp^*_2$(bipy) and $YbCp^*_2$(Me_2bipy). Analogous to their mononuclear cousins known for intermediate valence, spectroscopic evidence suggests that $YbCp^*_2$(bipy) features a multiconfigurational ground state, composed of a superposition of an open-shell ligand non-innocent $4f^{13}(\pi^*)^1$ state and a closed-shell $4f^{14}$ state. Our findings mark a first step toward increasing electronic correlations in lanthanide–organic frameworks, with the aim of realising materials with coexisting electronic transport and emergent magnetic properties.

Lanthanide chemistry has long been regarded as driven predominantly by ionic interactions due to the core-like nature of the 4f orbitals. Yet, a growing body of experimental and theoretical work has revealed the relevance of covalency for a multitude of properties.[1–3] Alternatively, strong covalency between lanthanide (Ln) ions and organic ligands implies comparable energies between the 4f and ligand valence orbitals.[4] Recently, we demonstrated that such a scenario in lanthanide–organic coordination solids may lead to distinct redox isomers in close energetic proximity, switchable by mild stimuli.[5–7] All experimental evidence in these systems point to integer Ln(II) or Ln(III) oxidation states. This result stands in contrast to previously established families of Ce and Yb molecular complexes.[8–11] In the case of the Yb complexes, the ground-state electronic wavefunctions are instead best described as multiconfigurational superpositions of e.g. f^{14} and $f^{13}(\pi^*)^1$, reflecting formal Yb(II) and Yb(III) oxidation states. Whilst this behaviour is also well-established in inorganic solids,[12–14] no extended metal–organic solids have been reported to parallel this electronic picture.

Complexes of ytterbocenes with redox-active ligands serve as paradigms of molecular intermediate valence.[10] Andersen and co-workers first reported electronic and magnetic anomalies in $YbCp^*_2$(2,2′−bipyridine) (Cp^{*-} = pentamethylcyclopentadienide) complexes in the early 2000s,[15] with later studies finding analogous behaviour in complexes featuring similar ligands such as phenanthroline, diazabutadiene, and substituted bipyridines.[9,16–20] These systems are distinguished by open-shell ground states, with magnetic moments varying wildly, and possible relevance of strong superexchange effects. However, direct evidence against a pristine Yb(III) state comes from Yb L_3-edge XANES, which reflect a multiconfigurational ground state, as evidenced by the co-existence of spectroscopic fingerprints of both Yb(II) and Yb(III). This leads to non-integral f-electron holes, typically between 0.8 and 0.95.[18,21] Multiconfigurational quantum chemical methods have identified the low-lying energy levels and quantified the admixture of $f^{13}(\pi^*)^1$ and f^{14} configurations.[9] Despite the large number of reported compounds, including polynuclear systems with ditopic ligands,[22,23] all verified examples of intermediate valence in ytterbocene chemistry have been limited to discrete complexes.

Extending redox-active metallocene units into polymeric frameworks presents a compelling opportunity. Firstly, the dimensionality may engender cooperative electronic effects in the bulk material, such as magnetic exchange coupling and charge transport pathways. Secondly, the rigidified polymeric environment may stabilize energetically adjacent intermediate valence configurations, switchable by temperature, which provide prospectives for e.g. metal–insulator transitions in lanthanide–organic networks. Motivated by these possibilities, we have synthesized and crystallographically characterised coordination solids composed of archetypal $YbCp^*_2$ units and by

[a] Department of Chemistry, Technical University of Denmark, Kemitorvet, DK-2800 Kgs. Lyngby, Denmark; E-mail: majdu@kemi.dtu.dk (M.A.D.), kastp@kemi.dtu.dk (K.S.P.)
[b] European Synchrotron Radiation Facility, 38000 Grenoble, France.
[c] Department of Chemistry, University of Copenhagen, DK-2100 Copenhagen, Denmark.
[d] LCM, CNRS, Ecole Polytechnique, Institut Polytechnique de Paris, 91120 Palaiseau, France.

† Electronic supplementary Information available. CCDC 2473188-2473189. For ESI and crystallographic data in CIF or other electronic format see DOI: 00.0000/00000000.

View Article Online
DOI: 10.1039/D5CC04048E

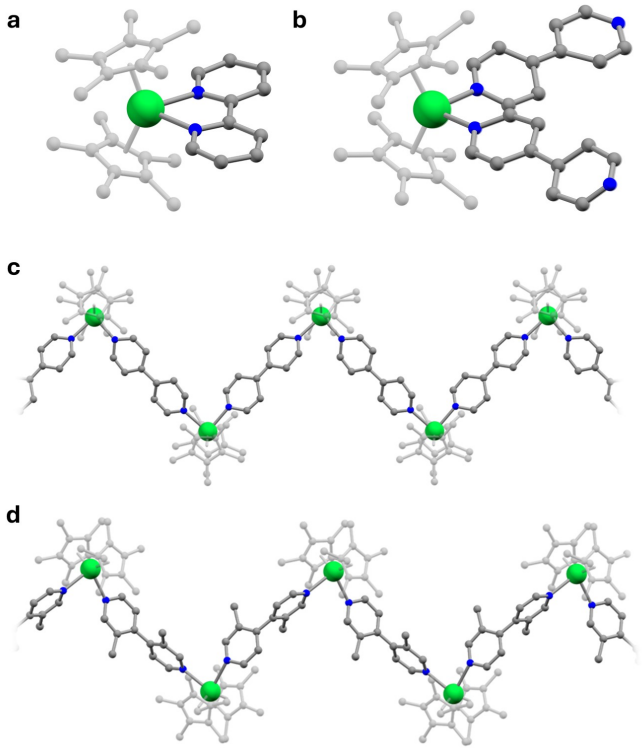

Fig. 1 Comparison of the first coordination spheres of (a) mononuclear intermediate valence compound $YbCp^*_2(2,2'-bipy)$ and (b) polymeric $YbCp^*_2(bipy)$. Extended zig-zag chains of (c) $YbCp^*_2(bipy)$ and (d) $YbCp^*_2(Me_2bipy)$. Colour code: Yb, green; N, blue; C, grey. Hydrogen atoms have been omitted for clarity.

4,4′−bipyridines, known for their redox plasticity in lanthanide compounds.[24–26]

The reaction of $YbCp^*_2(Et_2O)$ and 4,4′-bipyridine (hereafter called "bipy") in diethyl ether solution was first reported by Berg et al.[27] The resulting material was found to be insoluble and exhibited a high melting point, indicative of a polymeric structure, which at the time could not be unravelled. Using a different approach, we found that the solvent-free reaction of $YbCp^*_2(Et_2O)$ with bipy or 3,3′-dimethyl-4,4′-bipyridine (Me_2bipy) in a sealed ampoule at 150°C yields microcrystalline, dark-coloured materials. The crystallites obtained directly from the reaction vessels were suitable for structural characterization by single-crystal X-ray diffraction analysis. $YbCp^*_2(bipy)$ crystallizes in the monoclinic $P2_1/n$ space group, with two formula units per asymmetric unit, while $YbCp^*_2(Me_2bipy)$ crystallizes in $P2_1/c$ with one formula unit per asymmetric unit. Both structures feature $\{YbCp^*_2\}$ units bridged by the ditopic bipy ligands, forming one-dimensional chains in a zig-zag pattern (Figure 1c,d, Figures S1–4). Notably for $YbCp^*_2(bipy)$, the first coordination sphere, $YbCp^*_2L_2$, is directly analogous to that of the known intermediate valence compound $YbCp^*_2(2,2'-bipy)$ (Figure 1a,b; Yb−Cp* = 2.342(5) Å, 2.32(2) Å and Yb−N = 2.320(7) Å, 2.33(3) Å for $YbCp^*_2(2,2'-bipy)$ and $YbCp^*_2(bipy)$, respectively). Powder X-ray diffraction reveals that $YbCp^*_2(bipy)$ is obtained as a phase-pure material (Figure S5). However, in the reaction with Me_2bipy, a monophasic bulk material could not be obtained, despite extensive screening of reaction conditions (Figure S6).

For $YbCp^*_2L$ compounds, metal–ligand distances are dependent on the relative valence of Yb and ligand. The two compounds are here compared to $(Yb^{II}Cp^*_2(py)_2)$[9] and $[Cp^*Yb^{III}(2,2'-bipy)]^+$).[15] The metal–ligand distances of $YbCp^*_2(Me_2bipy)$ are characteristic of an Yb(II) oxidation state, evidenced by the distance between the Yb and the Cp* ring centroids of 2.453(7) Å (Yb(II): 2.466(1) Å; Yb(III): 2.301(2) Å), and the average Yb−N bond lengths of 2.55(1) Å (Yb(II): 2.565(1) Å; Yb(III): 2.372(3) Å). In comparison, for $YbCp^*_2(bipy)$, the bond lengths are closer to those of the Yb(III) reference, with Yb−Cp* of 2.32(3) Å and Yb−N of 2.33(3) Å. Due to large estimated standard deviation on the bond lengths in $YbCp^*_2(bipy)$, comparison of the interpyridinic C−C bond lengths is not warranted. However, for $YbCp^*_2(Me_2bipy)$, the interpyridinic C−C bond length is 1.48(2) Å, consistent with the presence of neutral Me_2bipy, rather than $Me_2bipy(\cdot-)$.[24,28] Additionally, both bipyridines in the asymmetric unit of $YbCp^*_2(bipy)$ maintain a near planar geometry, with only a slight 13(1)° interpyridinic torsion commensurate with a one-electron reduction of the ligand.[28] On the contrary, for $YbCp^*_2(Me_2bipy)$, the methyl sterics result in a torsion angle of 85.8(5)°, incompatible with any radical character of this ligand (Figure 1). Therefore, the structural analysis suggests a formulation of Yb(II)−bipy(0) in $YbCp^*_2(Me_2bipy)$, while $YbCp^*_2(bipy)$ reflects the Yb(III)−bipy(·−) tautomer.

To substantiate the oxidation state assignment in $YbCp^*_2(bipy)$, X-ray absorption near-edge structure (XANES) spectra were obtained around the Yb L_3 ($2p_{3/2} \longrightarrow 5d_{3/2,5/2}$) edge (Figure 2, Figure S7). The molecular precursor, $YbCp^*_2(Et_2O)$, serves as a pristine example of an Yb(II) complex, exhibiting an intense peak ("white line") energy of 8944 eV, while the established Yb(III) reference $[YbCp^*_2(2,2'-bipy)]I$ exhibits a 7 eV shift of the white line to 8951 eV, consistent with a one-electron oxidation.[9,19,20,29,30] The spectrum of $YbCp^*_2(bipy)$ is dominated by a white line at 8951 eV, confirming a predominant Yb(III) oxidation state. However, compared to the Yb(III) reference, $YbCp^*_2(bipy)$ features a distinct shoulder at the low-energy side of the white line. Indeed, a strikingly similar spectral fingerprint and temperature independence (Figure S8) are seen in the spectrum of the classic intermediate valence compound $YbCp^*_2(2,2'-bipy)$ (Figure 2), with an effective Yb(2.8+) oxidation state[18,21]. Qualitatively, $YbCp^*_2(bipy)$ exhibits a similar degree of mixed Yb(II)/Yb(III) character. An overlay of the weighted spectra of the Yb(II) (25%) and Yb(III) (75%) reference spectra with the spectrum of $YbCp^*_2(bipy)$ demonstrates how the resultant spectrum can be reproduced as a superposition of the two oxidation states. The presence of two crystallographically independent Yb sites could be a reason for the observed non-integer oxidation state (commonly interpreted as a mixed valence) as recently reported in $\{Yb_2\}$ dinuclear complexes;[30,31] however, the effective oxidation state as determined by XANES, and the structural similarity of the two sites, suggests instead a multiconfigurational ground state consistent with intermediate valence.

View Article Online
DOI: 10.1039/D5CC04048E

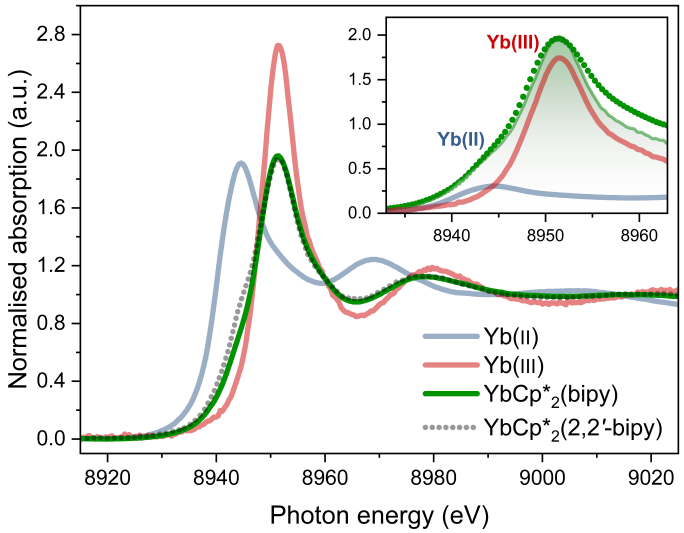

Fig. 2 X-ray absorption spectra of $YbCp^*_2$(bipy) (green), Yb(II) reference ($YbCp^*_2(Et_2O)$; blue), Yb(III) reference ([$YbCp^*_2$(2,2′−bipy)]I; red), and intermediate valence compound $YbCp^*_2$(2,2′−bipy) (grey dashed), obtained at the Yb L_3-edge (T = 295 K). Inset shows an overlay of the $YbCp^*_2$(bipy) spectrum (green data points) with a linear combination of the Yb(II) and Yb(III) reference spectra (25:75 ratio; Yb(II): blue line, Yb(III): red line, sum: green line).

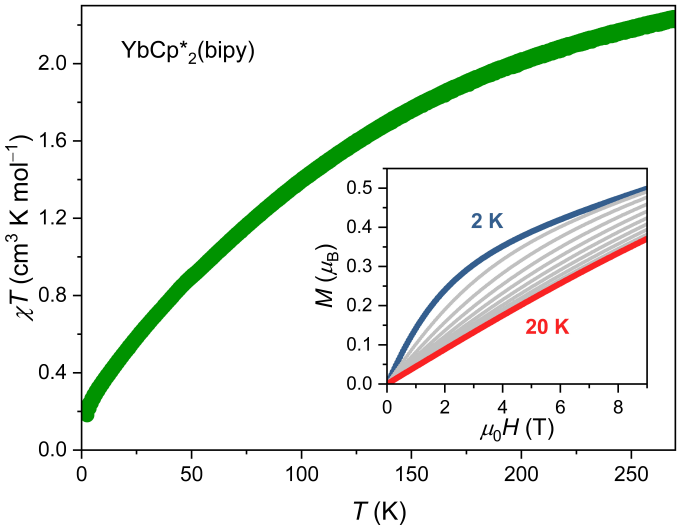

Fig. 3 Temperature dependence of the χT product at 0.1 T for polycrystalline $YbCp^*_2$(bipy). Inset: Magnetic field-dependence of the magnetization of $YbCp^*_2$(bipy) at temperatures between 2 K (blue) and 20 K (red) in 2 K increments, between 0 T and 9 T.

Intermediate valence Yb compounds often display intense absorption features in the near-infrared (NIR) spectral regime distinct from the weak f-f transitions typically observed for Yb(III) compounds (900–1100 nm; $^2F_{5/2} \longleftarrow {}^2F_{7/2}$).[15] The diffuse reflectance spectrum of the dark red-brown $YbCp^*_2$(bipy) (Figure S9) shows several bands in the visible region, ascribed to ligand-based transitions. In the NIR, a broad band at 1,580 nm (6,330 cm^{-1}), as well as weaker features at 940 and 984 nm (10,638, 10,163 cm^{-1}) are observed. These spectral features are notably different to those of the Yb(III) reference [$YbCp^*_2$(2,2′−bipy)]I, which features characteristically sharp f-f transitions.[15,32] This suggests a deviation from a pure Yb(III) valence in $YbCp^*_2$(bipy). Furthermore, the 5 K X-band electron paramagnetic resonance spectrum of $YbCp^*_2$(bipy) displays broad, but qualitatively similar features to that of the Yb(III) reference [$YbCp^*_2$(2,2′−bipy)]I, but distinct from the reported Yb(III)−L(·−) compound $YbCp^*_2$(phenanthroline) (Figure S11).[20]

The temperature dependence of the magnetic susceptibility–temperature product, χT, of $YbCp^*_2$(bipy) is shown in Figure 3. In the case of an Yb(II)−bipy(0) tautomer, the $4f^{14}$ configuration of Yb(II) would lead to a diamagnetic state. Alternatively, for a system comprising one Yb(III) ($^2F_{7/2}$, g_J = 8/7; C = 2.57 cm^3 K mol^{-1}) and one bipy(·−) radical (C = 0.375 cm^3 K mol^{-1}), an uncorrelated system would have a χT saturating at ∼2.9 cm^3 K mol^{-1}. The χT product value of $YbCp^*_2$(bipy) reaches instead only 2.2 cm^3 K mol^{-1} at 270 K. Upon cooling, the χT product decreases to reach ∼0.2 cm^3 K mol^{-1} at 2 K. Variable-field magnetization measurements of $YbCp^*_2$(bipy) in the temperature range from 2 to 20 K suggest the absence of a well-isolated magnetic ground state. The reported magnetic behaviour of $YbCp^*_2$(L) materials typically varies between those expected for the limiting Yb(II)−L(0) and Yb(III)−L(·−) cases,[9] and for $YbCp^*_2$(bipy) the observed magnetic data are consistent with an intermediate valence system behaving closer to an Yb(III)−L(·−) scenario. Recent reports on mixed-valent lanthanide molecular materials have shown remarkable magnetic properties, such as record-breaking coercive fields and high blocking temperatures.[1,33] To probe for the presence of any slow relaxation of magnetization, ac magnetic susceptibility measurements were performed at 1.8 K (Fig. S12). Even in applied magnetic fields up to 2 T, at 1.8 K $YbCp^*_2$(bipy) shows only rapid paramagnetic relaxation (ν_{max} > 10,000 Hz).

In summary, we report the first structurally characterized one-dimensional coordination solids constructed from ytterbocenes linked by organic ligands. Analogous to the propensity for mononuclear $YbCp^*_2$(L) complexes to exhibit multiconfigurational ground states, our data indicate a non-integer Yb valence in $YbCp^*_2$(bipy). The presence of such an intermediate valence in a polymeric molecular material is the first of its kind. Furthermore, the successful integration of redox-active $YbCp^*_2$ units into 1D frameworks could lead to the realization of materials properties novel to molecule-based materials. We conjecture that such materials with strong metal-ligand entangled electronic ground states may provide a possibility for through-bond electronic transport in f-element–organic networks, although this first example features a room temperature conductivity of just ∼ 10^{-9} S cm^{-1}.

Acknowledgements

K.S.P. thanks the Villum Foundation for a VILLUM Young Investigator+ (42094) grant, and the Independent Research Fund Denmark for a DFF-Sapere Aude Starting Grant (0165-00073B), and the Carlsberg Foundation for a research infrastructure grant (CF17-0637). K.S.P. and E.L. thank DTU for an Alliance PhD Fel-

View Article Online
DOI: 10.1039/D5CC04048E

lowship to E.L. This work was supported by the Danish National Committee for Research Infrastructure (NUFI) through the ESS-Lighthouse Q-MAT and the Danish Agency for Science, Technology, and Innovation through the instrument centre "Danscatt". The X-ray spectroscopy experiments were performed at the ID12 beamline at the European Synchrotron Radiation Facility (Grenoble, France). We acknowledge the Copenhagen Pulse-EPR Facility financed b y r esearch g rant N NF21OC0068806 R esearch Infrastructure - Large Equipment and Facilities 2021 by the Novo Nordisk Foundation.

Conflicts of interest

There are no conflicts to declare.

Data availability

The data supporting this article have been included as part of the Supplementary Information. Deposition Numbers 2473188-2473189 contain the supplementary crystallographic data for this paper. These data can be obtained free of charge via the joint Cambridge Crystallographic Data Centre (CCDC) and Fachinformationszentrum Karlsruhe Access Structures service

Notes and references

1 C. A. Gould, K. R. McClain, D. Reta, J. G. C. Kragskow, D. A. Marchiori, E. Lachman, E.-S. Choi, J. G. Analytis, R. D. Britt, N. F. Chilton, B. G. Harvey and J. R. Long, *Science*, 2022, **375**, 198–202.

2 F. Liu, G. Velkos, D. S. Krylov, L. Spree, M. Zalibera, R. Ray, N. A. Samoylova, C.-H. Chen, M. Rosenkranz, S. Schiemenz, F. Ziegs, K. Nenkov, A. Kostanyan, T. Greber, A. U. B. Wolter, M. Richter, B. Büchner, S. M. Avdoshenko and A. A. Popov, *Nat. Commun.*, 2019, **10**, 571.

3 P. Zhang, R. Nabi, J. K. Staab, N. F. Chilton and S. Demir, *J. Am. Chem. Soc.*, 2023, **145**, 9152–9163.

4 R. G. Denning, J. Harmer, J. C. Green and M. Irwin, *J. Am. Chem. Soc.*, 2011, **133**, 20644–20660.

5 M. A. Dunstan, A. S. Manvell, N. J. Yutronkie, F. Aribot, J. Bendix, A. Rogalev and K. S. Pedersen, *Nat. Chem.*, 2024, **16**, 735–740.

6 M. A. Dunstan and K. S. Pedersen, *Chem. Commun.*, 2025, **61**, 627–638.

7 A. Viborg, M. A. Dunstan, N. J. Yutronkie, A. Chanda, F. Trier, N. Pryds, F. Wilhelm, A. Rogalev, D. Pinkowicz and K. S. Pedersen, *Chem. Sci.*, 2025, **16**, 6879–6885.

8 M. D. Walter, C. H. Booth, W. W. Lukens and R. A. Andersen, *Organometallics*, 2009, **28**, 698–707.

9 C. H. Booth, D. Kazhdan, E. L. Werkema, M. D. Walter, W. W. Lukens, E. D. Bauer, Y.-J. Hu, L. Maron, O. Eisenstein, M. Head-Gordon and R. A. Andersen, *J. Am. Chem. Soc.*, 2010, **132**, 17537–17549.

10 M. Tricoire, N. Mahieu, T. Simler and G. Nocton, *Chem. Eur. J.*, 2021, **27**, 6860–6879.

11 M. A. Hay and C. Boskovic, *Chem. Eur. J.*, 2021, **27**, 3608–3637.

12 V. N. Antonov, L. V. Bekenov and A. N. Yaresko, *Adv. Condens. Matter Phys.*, 2011, **2011**, 298928.

13 S. F. Matar, *Prog. Solid State Chem.*, 2013, **41**, 55–85.

14 S. Engel, E. C. J. Gießelmann, M. K. Reimann, R. Pöttgen and O. Janka, *ACS Org. Inorg. Au*, 2024, **4**, 188–222.

15 M. Schultz, J. M. Boncella, D. J. Berg, T. D. Tilley and R. A. Andersen, *Organometallics*, 2002, **21**, 460–472.

16 M. D. Walter, M. Schultz and R. A. Andersen, *New J. Chem.*, 2006, **30**, 238–246.

17 M. D. Walter, D. J. Berg and R. A. Andersen, *Organometallics*, 2006, **25**, 3228–3237.

18 C. H. Booth, M. D. Walter, D. Kazhdan, Y.-J. Hu, W. W. Lukens, E. D. Bauer, L. Maron, O. Eisenstein and R. A. Andersen, *J. Am. Chem. Soc.*, 2009, **131**, 6480–6491.

19 G. Nocton, C. H. Booth, L. Maron and R. A. Andersen, *Organometallics*, 2013, **32**, 1150–1158.

20 G. Nocton, W. W. Lukens, C. H. Booth, S. S. Rozenel, S. A. Medling, L. Maron and R. A. Andersen, *J. Am. Chem. Soc.*, 2014, **136**, 8626–8641.

21 C. H. Booth, M. D. Walter, M. Daniel, W. W. Lukens and R. A. Andersen, *Phys. Rev. Lett.*, 2005, **95**, 267202.

22 C. N. Carlson, C. J. Kuehl, R. E. Da Re, J. M. Veauthier, E. J. Schelter, A. E. Milligan, B. L. Scott, E. D. Bauer, J. D. Thompson, D. E. Morris and K. D. John, *J. Am. Chem. Soc.*, 2006, **128**, 7230–7241.

23 H. Gupta, A. Sen, P. W. Smith, B. D. Vincenzini, N. Mavragani, D.-C. Sergentu, A. M. Bacon, C. H. Booth, M. Murugesu, S. G. Minasian, J. Autschbach and E. J. Schelter, *Inorg. Chem.*, 2025, **64**, 14753–14758.

24 L. Voigt, M. Kubus and K. S. Pedersen, *Nat. Commun.*, 2020, **11**, 4705.

25 H. Chen, L. Voigt, M. Kubus, D. Mihrin, S. Mossin, R. W. Larsen, S. Kegnæs, S. Piligkos and K. S. Pedersen, *J. Am. Chem. Soc.*, 2021, **143**, 14041–14045.

26 H. Chen, A. S. Manvell, M. Kubus, M. A. Dunstan, G. Lorusso, D. Gracia, M. S. B. Jørgensen, S. Kegnæs, F. Wilhelm, A. Rogalev, M. Evangelisti and K. S. Pedersen, *Chem. Commun.*, 2023, **59**, 1609–1612.

27 D. J. Berg, J. M. Boncella and R. A. Andersen, *Organometallics*, 2002, **21**, 4622–4631.

28 M. S. Denning, M. Irwin and J. M. Goicoechea, *Inorg. Chem.*, 2008, **47**, 6118–6120.

29 G. Nocton, C. H. Booth, L. Maron and R. A. Andersen, *Organometallics*, 2013, **32**, 5305–5312.

30 M. D. Roy, T. P. Gompa, S. M. Greer, N. Jiang, L. S. Nassar, A. Steiner, J. Bacsa, B. W. Stein and H. S. La Pierre, *J. Am. Chem. Soc.*, 2024, **146**, 5560–5568.

31 T. J. N. Obey, M. K. Singh, A. B. Canaj, G. S. Nichol, E. K. Brechin and J. B. Love, *J. Am. Chem. Soc.*, 2024, **146**, 28658–28662.

32 R. E. Da Re, C. J. Kuehl, M. G. Brown, R. C. Rocha, E. D. Bauer, K. D. John, D. E. Morris, A. P. Shreve and J. L. Sarrao, *Inorg. Chem.*, 2003, **42**, 5551–5559.

33 H. Kwon, K. R. McClain, J. G. C. Kragskow, J. K. Staab, M. Ozerov, K. R. Meihaus, B. G. Harvey, E. S. Choi, N. F. Chilton and J. R. Long, *J. Am. Chem. Soc.*, 2024, **146**, 18714–18721.

View Article Online
DOI: 10.1039/D5CC04048E

Data availability statement

The data supporting this article have been included as part of the Supplementary Information. Deposition Numbers 2473188-2473189 contain the supplementary crystallographic data for this paper. These data can be obtained free of charge via the joint Cambridge Crystallographic Data Centre (CCDC) and Fachinformationszentrum Karlsruhe Access Structures service.